




Allocation of Promising Objects for a Group of Deposits in the Karagay Saddle



Mansiya Yessenamanova^{1*}, Gulbanu Zhiyenbayeva², Kossarbay Kozhakhmet², Maxat Tabylganov², Salima Cherkeshova², Nursaule Tauova², Zhanar Yessenamanova¹, Anar Tlepbergenova¹

¹ Ecology Department, Kh.Dosmukhamedov Atyrau University, 060001 Atyrau, Republic of Kazakhstan

² Department of Ecology and Geology, Sh.Yessenov Caspian University of Technology and Engineering, 130000 Aktau, Republic of Kazakhstan

* Correspondence: Mansiya Yessenamanova (m.esenamanova@asu.edu.kz)

Received: 06-12-2022

Revised: 07-11-2022

Accepted: 07-28-2022

Citation: M. Yessenamanova, G. Zhiyenbayeva, K. Kozhakhmet, M. Tabylganov, S. Cherkeshova, N. Tauova, Z. Yessenamanova, and A. Tlepbergenova, "Allocation of promising objects for a group of deposits in the Karagay saddle," *Acadlore Trans. Geosci.*, vol. 1, no. 1, pp. 33-42, 2022. <https://doi.org/10.56578/atg010105>.



© 2022 by the author(s). Published by Acadlore Publishing Services Limited, Hong Kong. This article is available for free download and can be reused and cited, provided that the original published version is credited, under the CC BY 4.0 license.

Abstract: This work completes the thorough petrophysical interpretation of 46 wells, as well as a technical feasibility analysis. Even though the acoustic logging was of very poor quality, work was done to get it ready for use in creating synthetic seismograms that accurately represented the section. The sle.28 Karagie Severny, which was drilled in 2012 and has significantly better GIS quality, was used to control this operation. Through a dynamic analysis, the shooting system's (footprint) influence on the distribution of the amplitudes at the Karagie Severny site was not eliminated during data processing, but it was removed during the re-processing. As a result, the findings for Karagie Severny should be taken with a grain of salt because the initial data's quality was not considered when choosing the sites for the suggested wells. However, the seismic facies analysis in two forms—classical and cluster—showed the presence of at least three primary facies complexes, which are reflected in both formed, with a more precise distribution in accordance with cluster analysis.

Keywords: Horizon; Wells; Seismic inversion; Karagay saddle

1. Introduction

Administratively, the oil fields of the Karagie Severny, Ashchiagar, Alatyube, and Atambai-Sartyube are situated close to the Caspian Sea in the Karakiya district of the Mangystau region of the Republic of Kazakhstan (Figure 1) [1]. The fields are 20–40km away from the Aktau regional center. Orographically, the region is composed of a variety of surface reliefs, including minor flat regions, sediment zones, and the remains that lie beneath high scarp slopes in the northern section of the Karagiye depression. The depression's lowest point is occupied by the Batyr Sor. The range of ground elevations is -105 to +100m. The Karagie Severny, Alatyube, and Ashchiagar deposits are positioned in the most submerged region of Karagiye Depression in the north, with an elevation range of -102 m to -55 m. Heterogeneity exists on the relief surface, which is covered by limestones, sandy loams, loam soils, and heterochronous sands. The western portion of the site, where negative elevations of the relief shift to positive, is where the Atambai-Sartyube field is located. It lies along the western edge of the depression within the slope.

The Alatyube, Atambay-Sartyube, Ashchiagar, and Karagie Severny deposits are located inside the Karagi saddle, which is a tectonic feature of the II order. The Segendyk depression, in the west, the Segendymys stage, in the north, the Zhetybai-Uzen stage, in the north-east and east, the Zhazgurli depression, in the south-east, and the Peschanomyssko-Shell zone of vaulted uplifts, in the south—all meet at the Karagi saddle.



Figure 1. Survey map of the research area

The research area (Figure 1) is intriguing since it lies where the Large Mangyshlak fault and the Karagi saddle meet. These faults predicted the zones of distribution of high fracturing, as shown by the high flow rates in the wells of the nearby Alatube field.

The Jurassic-Triassic rock complex is linked to the primary potential for oil and gas resources. The Zhetybai, Akkar Severny, Zhetybai North-Western, and other fields have been found on the area bordering the examined territory [2].

The exploration of Mangyshlak's hydrocarbon potential saw the discovery of rare oil and gas reserves including Zhetybai (1961) and Uzen (1962). Several tiny oil and gas concentrations were found in the thickness of the Jurassic layers during further geological exploration, but such substantial accumulations were no longer present. In the 1950s, the geological and geophysical research of Mangyshlak [3] initiated a differentiated assessment of the chances for oil and gas content, and provided a strategy for prospecting and exploring activities. Up to the 1960s, the planned complex of geological and geophysical works was completed. According to the findings of a high-precision aeromagnetic survey (1956-1958) and a gravimetric survey (1958), maps of magnetic anomalies and gravity anomalies were constructed at a scale of 1: 200,000. Additionally, in the modern South Mangyshlak oil province, reconnaissance and then in-depth seismic investigation using the 2D seismic reflection method were conducted on a scale of 1: 100,000 at the three most prospective rises: Zhetybai (1957-1958), Uzen, and Eastern Zhetybai (1959-196). These findings led to the drilling of deep wells and the unique Southern Mangyshlak oil and gas fields of Zhetybai (1961) and Uzen (1962), which were found in the Jurassic layers.

2. Methodology

Scientific research and production work on the investigation of the geological structure and oil and gas potential of the Southern Mangyshlak in general, and the Zhetybai-Uzen tectonic stage in particular, intensified over the years, particularly in the 1960s. The thickness of the Jurassic deposits was found to contain a number of tiny oil and gas through geological exploration, but such massive accumulations as the original deposits were no longer present [4].

By the end of the 1970s, 20 out of the 42 known fields in the South Mangyshlak oil and gas region had been located; 14 of these were oil and gas fields and 6 were gas fields. Triassic deposits only had one deposit established (S.Z. Zhetybay). In three more deposits (Y. Zhetybai, Tasbulat, and Rakushechnoye), the productivity of Triassic deposits and the productivity of Jurassic deposits were both established. As the supply of structures in the Jurassic reservoirs ran out, drilling began on deeper and more tectonically dislocated structures in the Triassic deposits.

A regional structural basis for Triassic deposits was produced based on an examination and generalization of common depth point technique materials in 1978 on the entire South-Mangyshlak oil and gas region [5]. Additionally, the tectonic structure of the area was described, revealing that the roofing portions of the Lower, Middle, and Upper Triassic deposits contain angular disagreements. These resources provided the framework for the initial exploration of Triassic deposits [6].

Geological investigation was carried out up to the end of the 1990s, leading to the discovery of an additional 21 fields, of which 15 were gas and oil fields and 6 were gas fields, with 17 being discovered in the 1980s and just 4 in the 1990s. There were found to be 14 deposits, including those from the Triassic. The Akkar North oil field, which is also restricted to Triassic deposits, was added to them in the 2000s.

In 1989, an object in the first well (No. 1) was tested in the Middle Triassic deposits, leading to the discovery of the Atambay-Sartyube field. The Middle Triassic deposits were sampled in order to establish the oil deposit, from which an industrial oil inflow was derived. Due to thorough seismic investigations, the structure and another uplift, Ashchiagar, were readied for drilling in 1988. Due to the drilling of well 1 Ashchiagar at the end of 1990,

a flow was also acquired from the Middle Triassic deposits, leading to the discovery of the Ashchiagar field. In 1993, the field had an experimental surgery.

Tables 1-4 explain the variables and procedures of seismic surveying of these fields [7].

Table 1. Layout

№	Parameter name	Values
1.	Total multiplicity	66
2.	Bin size [m×m]	25×25
3.	Number of receiver lines (RLs) in the band	12
4.	Number of receiver points (RPs) on the RL	88
5.	Number of live channels	1056
6.	RPs steps on RL [m]	50
7.	RL spacing [m]	200
8.	Far source-receiver offset	2745
9.	Location of shot point line	Cross spread
10.	Number of shot points on shot point line	24
11.	Shot point step on shot point line [m]	50
12.	Spacing of shot point line [m]	200

Table 2. Source parameters

№	Parameter name	Values
1	Total signal source points on survey area	18488
2.	Transmission method (85 %)	vibration
3.	Vibrator type	Nomad-65
4.	Number of vibrators	2
5.	Number of accumulations	2
6	Sweep frequency bandwidth	8-112 hz, 14-112 hz
7	Taper	1500 ms
8	Sweep length	10 s
9	Peak ground force	70%
10	Transmission method (15 %)	exploding
11	Type of excitation	БТН-500
12	Charge weight, shot depth	0.5 kg; 12 m

Table 3. Receiver parameter

№	Parameter name	Values
1.	Type of geophones	GS-20DX
2	Number of geophones per route	12
3	Length of grouping base [m].	24,97

Table 4. Recording parameters

№	Parameter name	Values
1.	Type of seismic station	I/O Scorpion
2	Recording length; sampling frequency	5s; 2 ms
3	Tape format	SEGY

A pair is ideal for mixed-type deposits, but in this case, it was vital to consider the method's existence, which was frequently not registered.

In light of the findings of the analysis of core samples, the accuracy of the quantitative parameter calculations (C_p - porosity coefficient and C_s - oil saturation coefficient) was checked.

Complex acoustic, neutron, and density calculations were used to determine the porosity coefficient in terrigenous deposits [8].

The porosity C_p can be estimated by the acoustic technique:

$$C_p = \frac{\Delta T_f - \Delta T_r}{\Delta T_l - \Delta T_r} - C_c \frac{\Delta T_c - \Delta T_r}{\Delta T_l - \Delta T_r} \quad (1)$$

where, ΔT_f is interval time of the elastic wave running in the formation; $\Delta T_r = 174$ ms/m is interval time of the wave running through the rock (sandstone); $\Delta T_l = 590$ ms/m is the interval time of an elastic wave running in a

liquid; ΔT_c is the interval time of an elastic wave running in clays; C_c is the volume content of clay in the reservoir layer.

The porosity can also be estimated by the neutron method:

$$C_p = W - C_c \cdot W_c \quad (2)$$

where, W is the total water content; C_c is the volume content of clay in the reservoir layer; $W_c = 0.30$ is the volume content of bound water in clay.

The porosity can additionally be estimated by the density method:

$$C_p = \frac{\sigma_s - \sigma_f}{\sigma_s - \sigma_w} \quad (3)$$

where, $\sigma_s = 2.66 \text{ g/cm}^3$ is the skeletal density of sandstone; σ_f is the volume density of the counter-interpreted formation; $\sigma_w = 1 \text{ g/cm}^3$ is the density of reservoir water. The porosity values according to GIS vary in the range of 10-18%.

The oil saturation coefficient C_p can be determined by:

$$C_s = 1 - C_w \quad (4)$$

where, C_w is the water saturation coefficient:

$$C_w = \left(\frac{1}{P_s}\right)^n \quad (5)$$

where, P_s is the saturation parameter:

$$P_s = \frac{\rho_p}{\rho_w} \quad (6)$$

where, ρ_p is the electrical resistivity of the reservoir obtained by lateral and induction logging; ρ_w is the electrical resistivity of the aquifer, i.e., the empirical reservoir in the case of 100% saturation with water.

3. Results

To identify perspective objects in the software Petrel, conceptual models were built for all deposits identified within the group of deposits. The structural maps from the corresponding reflecting seismic horizons served as the basis for the models. On this basis, structural maps for the top and bottom of each of the productive horizons—T3, T2A, and T2B—productive within particular fields were made and linked with well data (Figure 2).

The location of the defined oil-water limits and the results of the tests were taken into consideration while building the reservoir models [9]. The geometrization of each deposit was finished based on these data and taking into account the location of the identified and potential tectonic faults. The position of the producing horizon's cap, base, and, most importantly, oil-water sections, were the structural factors that served as the foundation for reservoir models. In every instance, the established facts of oil saturation up to a certain level were considered to be the most crucial information. Additionally, the boundaries of the reservoir were established while taking into account the presence of a closed contour or, if the closed contour extended too far, shielding by tectonic faults.

The location of the wells from which oil inflows were acquired served as a guiding principle in the geometrization of deposits.

According to the location of the recognized and alleged violations, wells in which inflows were not received were not taken into consideration. In some cases, the inflows were shut off by violations in productive blocks while in other cases they were included in productive blocks. The provisions of the oil-water contact were implemented in accordance with the conclusions of the most recent reserve calculations, which were accepted. The review of GIS interpretation data also revealed that, in certain instances, the water contact may be less than what was indicated in the reports.

For instance, according to Ozdojev [10], there are significant prospects that the water-oil contact for the T3 and T2-A deposits (western block) may be lowered in the future by roughly 20m to -3887.3m and -3978.0m, respectively, within the Alatyube field. Unfortunately, the production of these deposits in well No. 7, from where these contacts are meant to be registered, was not confirmed by the test findings. As a result, for the Alatyube field, the water-oil contact is recognized for deposits T3, T2-A, and T2-B at elevations of -3860.0m, -3955.0m, and -3992.0m for the western block, respectively.

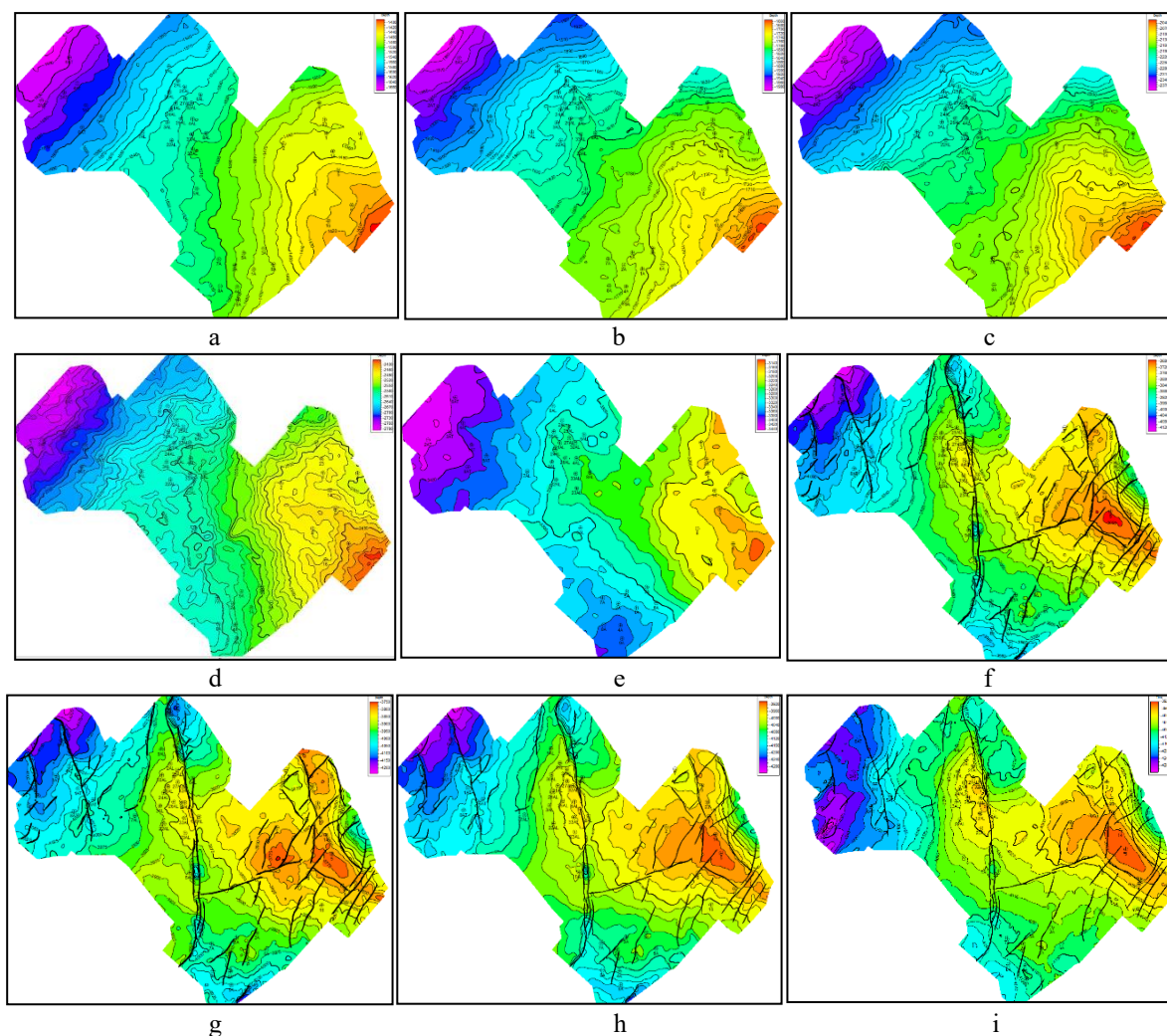


Figure 2. Structural map along the horizon: a) IIa, b) III, c) IIIa, d) IV, e) V₁, f) V₂, g) V₂^{II}, h) V₂^{IV}, i) VI

The water-oil contact of the T3 deposit was determined to be at -3874.0 m and 3943.0 m for the areas of wells 5–6 and well-8 in the Ashchiagar field. The water-oil contact in wells 7 and 9 may be located at a lower position of -3886.0 m and -3940.0 m, respectively, when the GIS interpretation results are taken into account.

According to the results of the GIS analysis for well No. 9, the oil-water contact of the T2-A deposit may not be -4031.0m as is accepted in the report on the calculation of reserves, but may instead be -4048.5m (well No. 9), which is accepted in the current work. The Ashiagar field's Horizon T2-B is inundated.

The Upper Triassic horizon of the Atambay-Sartyube field is regarded as unproductive. The basal horizon, which is typically referred to as the T3 horizon, is identified here in a number of wells by formations with good reservoir qualities. Thus, a 3.4m reservoir with a porosity of 20-25% and an oil saturation range of 0.45-0.76 is found in well No. 5 in the depth range of 3895.9–3899.3m (abs.-3923.1-3926.5m). In addition to this well, similar formations with good reservoir features and oil saturation are found in wells 1, 5, and 8 as well.

The oil-water contact of T2-B, the major productive horizon of the Atambay-Sartyube field, is taken at around -4192m. The higher water mark, established in well 6, is -4196 m, whereas the lower oil mark in well 3 is set at -4193.2 m. As a result, the water-oil contact may be accurately determined here and is likely to be at a level of -4194-95 m, which is near to the position that is currently accepted for it (-4192 m).

According to well 4, where an inflow of anhydrous oil was acquired from the interval 4040-4044m (-4050.9-4045.9m), the water-oil contact for the T2-A horizon at the Atambay-Sartyube field was taken at a depth of -4067.9m. The oil reservoir can be tracked to a depth of 4057m according to the GIS (-4067.9m).

The T3 horizon is the Karagie Severny field's most productive horizon. Two parts of the field are identified based on the level of oil-water contact: the western part (oil-water contact -3756.0m) and the eastern part (oil-water contact -3766.0m). A tectonic fault that separates the deposit can be seen by looking at the structural surface's shape. By analyzing the materials, the oil-water contact for the western part of the well may be taken at -3757.6m, where the oil part of the section can be traced to a depth of 3668.3m (-3757.6m). According to data from well No. 16, where the oil-saturated reservoir assigned by GIS was tested to the level of -3769.7 m and an

anhydrous inflow of oil with a flow rate of 1.0 m³ was obtained at the level of 1730 m, the water-oil contact can be accepted for the eastern part of the reservoir. The oil-water contact for the T2-B horizon was measured at -3900m for the western part and 3904m for the eastern part. Further analysis shows that the water-oil contact of both parts can be at the same level.

The productivity of the T2-A horizon merits special consideration because it was -3908.8 m according to the data from wells No. 1 and 2. There are no reservoirs in several wells in this horizon: 2, 4, 7, 16. The productivity is predicted by GIS to be up to -3827.0 m in wells where the horizon's Kp is 5-8% or more, which is established in well No. 14.

The conceptual models for each field employed the oil-water contact levels mentioned above. The location of potential development zones, including those with enhanced quality and a dearth of reservoirs, was determined using field reservoir models in conjunction with attribute and seismic facies maps.

There was no single attribute, seismic facies, or lithofacies map that could be used to clearly predict development reservoirs in productive Triassic deposits, as evidenced by studies on the study of various seismic attributes, seismic facies, both classical and cluster, sedimentological and lithofacies analyses, and the results of inversion.

In accordance with the outcomes of testing and development, it is possible to produce such a forecast in a specific region of the territory using a variety of derived features and maps that primarily rely on reflection amplitudes.

Ambiguities, as demonstrated by the analysis, are caused by the fact that, when using typical correlated horizons, some parts of the section are inevitably added when calculating parameters. This may have an impact on the distribution of characteristics or facies. As a result, a more thorough investigation of the seismic data within the section's productive area was required. With the current resolution of seismic data, the most detailed model was constructed for this purpose. Pre-Stack Time Migration software was used to automatically track all seismic peaks and troughs in the 3D data cube (Figure 3) [11].

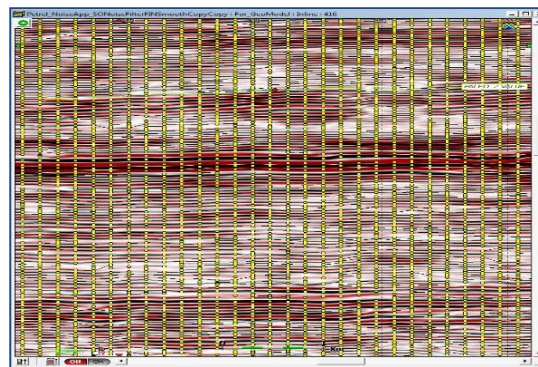


Figure 3. Seismic peaks and troughs in the 3D data cube

Additionally, the correlation coefficient-based traced reflections were automatically integrated into extended horizon sections, and the accuracy of the tracking was verified. Consequently, 207 extended horizons with sustained polarity were carefully gathered from various regions. The 3D data cube was converted into a relative geochronological model based on the structural framework that was created. Nine horizons, corresponding to the reservoir limits and describing the internal structure of the reservoirs, were traced across the thickness of the Triassic productive deposits.

Using a high-resolution spectral decomposition cube with 50Hz, 55Hz, and 60Hz frequency bands, the location of the Paleozoic deposits was refined (HDFD). The Paleozoic and overlying deposits' acoustic densities are different, hence the boundary between them may be seen in this cube rather clearly.

The parameters for the final forecast of reservoir growth within the intervals that correspond to the maximum extent of the investigated productive horizons in seismic were cluster seismic facies (stratimagic). The temporal sections that display the horizons between which the facies are distinguished and the change in the nature of the facies are colored to facilitate the identification of cluster facies. Then, future prospects were evaluated based on the outcomes of the development. This comparison is unclear, because production from the T2-A and T2-B horizons was done simultaneously without paying attention to the input location [12].

The fundamental issue with field development is the unpredictability of reservoir development, which used to be a deterrent because reservoir replacement zones were established by drilling data. The location and type of facies were influenced by facies circumstances during the creation of sediments. Fluvial channel and inter-channel valley facies are the defining features of deposits of the T3 horizon. For, T2B horizon, only the following are distinguished: one facies, the sandy shallow water of the inner ramp's peloid, bioclastic deposits. This is in contrast to the T2A horizon, which is distinguished by ooid and peloid sands, grain stones, as well as lagoon and tidal flat facies.

Along with this, the characteristics of the productive horizon's reflection in seismic data, brought on by secondary processes, particularly dolomitization, can also have an impact on the drawing of facies. Since the formation of structures within the area under consideration is characterized by an early (Late Triassic and pre-Early Jurassic) beginning of formation and only some renewal in the subsequent time, and in particular, the formation of the slope of the layers in a western direction, the influence of tectonic processes is expressed to a lesser extent [13].

4. Discussion

Based on the above results, the forecast for the development of deposits was mapped, taking account of both the structural factor and the reservoir development predicted by seismofacial studies. The location of the wells was chosen such as to open the most promising facies along one or another horizon within the oil zone, i.e., the T2-B Karagie Severny horizon within the vast water-oil zone. It is possible that this will also be an oil zone. The drilling of the wells listed in Table 5 is suggested in light of the above research. The area that could be used for deposit development is enormous, and the region's prospects could be greatly increased.

There are 16 fresh wells that should be drilled. In the region of the horizon T3 sandstones where porosity is at its highest and coincides with the uplift's crest, well 16PR is advised. Based on the distribution of seismic facies and lithofacies, further well locations were chosen. The facies of distributive channels, followed by that of mouth bars and coastal deposits, is the most ideal for the T3 horizon. The facies in the delta's distal portion are the least promising. Only wells No. 15 and 16 are advised for the T3 horizon; the other wells, which target carbonate deposits, will effectively penetrate Upper Triassic deposits; the best results can be anticipated from well No. 4 [14] (Figure 4).

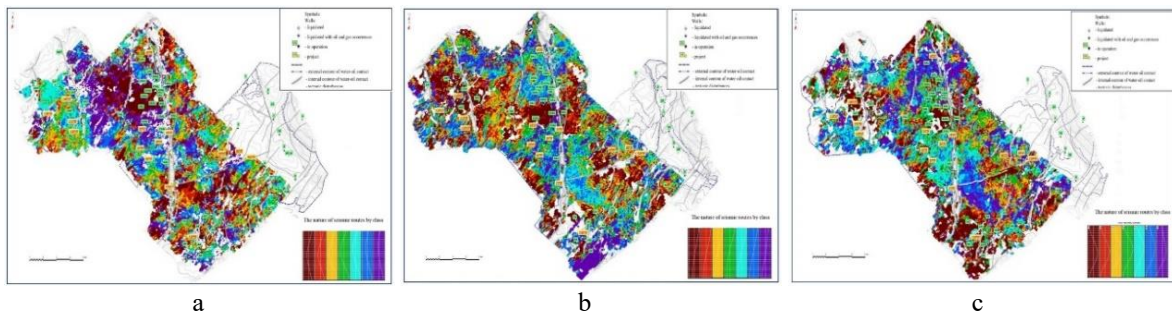


Figure 4. Position of the projected wells and contours of the Water-oil contact along the horizon: a - T3, b - T2, c - T2B

For the T2A horizon, it is advised to drill wells No. 1-7 Alatyube and No. 8-10 in the western section of Karagie Severny. Since the Alatyube is where these facies developed, the wells were also drilled on facies associated with the development of packstones and grainstones (well No. 4). The red zones on the map, for which wells are advised, demonstrate the ideal sites for reservoir development in the area of development of these facies that tend to grainstones. For each such site, potential reserves are determined (Table 5).

The Atanbay-Sartyube field's T2B horizon, which is represented by grainstones of the inner ramp, is best accessed by wells 11 to 14.

In addition, well No. 5 at the Ashchiagar field and wells No. 8-10 in the western part of the Karagie Severny field are advised for comparable facies. Furthermore, Table 5 demonstrates that the Alatyube field's suggested wells No. 3, 6, and 7 will open the T2B horizon in a favorable setting for the establishment of reservoirs. The forecast can serve as the basis for further research into the field, despite some doubts regarding the genuine resolution of the seismic data, the accuracy of the logging and testing, and the paucity of data on the input from each horizon.

The computation of reserves in the area of optimal facies development, for which the calculation parameters for each field and horizon were utilized, provides evidence of the economic effectiveness of drilling each well (Table 5).

In addition, the T2A horizon's effective thickness, which is equal to 22 meters in the well 32 Alatyube that exposed it, was used as a feature for this group of facies. Half of this value, or 10 meters, was used in the computations. Although the effective thickness for the T2B horizon is accepted to be the same as the T2A horizon despite the calculation showing otherwise, more conservative porosity coefficient values are used in the reserve calculation report than in the present work's GIS interpretation. The effective thickness average from the reserve count is used for the T3 horizon.

Table 5. Reserves attributable to the sites of the recommended wells

Field	Well	Horizon	Area of reservoir development area, thousand m ²	net pay of zone, m	Porosity, decimal quantity	Hydrocarbon charge, decimal quantity	Oil density, t/m ³	Conversion factor, decimal quantity	Geological oil reserves, thousand tons	Oil recovery index	Recoverable oil reserves, thousand tons
Alatyube	1	T2-A	606	5.0	0.07	0.70	0.835	0.752	92	0.300	28
	2		586	6.0	0.08	0.70	0.835	0.752	121	0.300	36
	3		893	6.0	0.08	0.70	0.835	0.752	192	0.300	58
	4		626	5.0	0.07	0.70	0.835	0.752	93	0.300	28
	5	T2-A	1005	6.0	0.08	0.70	0.835	0.752	206	0.300	62
		T2-B	792	10.0	0.13	0.70	0.848	0.824	504	0.300	151
	6	T2-A	649	6.0	0.08	0.70	0.835	0.752	135	0.300	40
7	627		6.0	0.08	0.70	0.835	0.752	140	0.300	42	
Total Alatyube									1483		445
Karagiye Severny	8	T2-A	2049	7.0	0.09	0.70	0.835	0.752	577	0.300	173
		T2-B	804	9.0	0.11	0.70	0.848	0.824	400	0.300	120
	9	T2-A	1014	7.0	0.09	0.70	0.835	0.752	285	0.300	86
		T2-B	1062	10.0	0.12	0.70	0.848	0.824	600	0.300	180
	10	T2-A	825	7.0	0.09	0.70	0.835	0.752	223	0.300	67
		T2-B	1087	9.0	0.11	0.70	0.848	0.824	519	0.300	156
Total Karagiye Severny									2605		782
Atambay	11	T2-B	589	7.0	0.11	0.70	0.848	0.752	201	0.250	50
	12	T2-B	800	10.0	0.11	0.70	0.819	0.722	369	0.250	92
	13	T2-B	495	10.0	0.11	0.70	0.819	0.722	232	0.250	58
	14	T2-B	1000	10.0	0.10	0.70	0.819	0.722	433	0.250	108
Total Atambay									1234		309
Aschiagar	15	T3	668	3.0	0.17	0.70	0.823	0.755	146	0.240	35
Total for the group of fields									5468		1570

Along with exploring the formation of reservoirs in the Triassic productive deposits, researchers also looked into the Jurassic and Cretaceous deposits above them. On these deposits, structural maps, attribute analyses, and logging analyses were developed.

Unfortunately, not all wells had logging data in the section's upper part. The investigation, however, revealed the absence of conditions in the region for the growth of structural traps in the Jurassic-Cretaceous sediment complex.

The development of lithological or combination traps is not ruled out by the results. With their arcuate orientation toward the rising of the strata, such traps may be connected to the Middle Jurassic channels that have been described. To investigate the potential productivity of Jurassic sandstones in such traps, more well data are still lacking. By building conceptual models of each deposit discovered within the set of deposits, it is possible to identify perspective objects in Petrel. The structural maps from the associated reflecting seismic horizons served as the models' foundation [15].

On this basis, structural maps for the top and bottom of each of the productive horizons—T3, T2A, and T2B—productive within particular fields were made and linked with well data.

The location of the defined oil-water limits and the results of the tests were taken into consideration while building the reservoir models. The geometrization of each deposit was finished based on these data and taking into account the location of the identified and potential tectonic faults. The position of the producing horizon's cap, base, and, most importantly, oil-water sections, were the structural factors that underpin the reservoir models. In every instance, the established facts of oil saturation up to a certain level were considered to be the most crucial information. Besides this, the boundaries of the reservoir were established while taking into account the presence of a closed contour or, if the closed contour extended too far, shielding by tectonic faults.

5. Conclusions

After converting the seismic to 0-phase form, a seismic inversion was performed, and impedance cubes with the best GIS quality were created while accounting for all wells. The results analysis allowed for the selection of a working cube, from which porosity maps for the T3, T2A, and T2B horizons were calculated using dependencies discovered during the feasibility analysis. These porosity maps demonstrated good convergence with well data, particularly for the T2B horizon.

Further, the authors compared the chosen facies fields with well performance, and demonstrated that the facies of erosion cuts for the T3 horizon and the facies of increasing thickness for the T2B horizon are the best in this regard (Severny Karagiye).

Given the uncertainty in the forecast, it is advised to drill wells in the areas in a particular order, laying new ones after getting the results from the previous ones. In this way, it is possible to validate the accuracy of the forecast.

Special consideration should be given to the T2A horizon since very good reservoirs can be produced there, which are frequently linked to karstification and leaching. New well recommendations were made in the most promising regions. Following their confirmation, further field locations that are prospective for new wells can be found, particularly along the Karagiye Severny (horizon T3), where several areas of increasing porosity are identified.

Author Contributions

The contributions of each author in the following statement: “Conceptualization, Mansiya Yessenamanova and Kossarbay Kozhakhmet; methodology, Kossarbay Kozhakhmet; software, Anar Tlepbergenova; validation, Kossarbay Kozhakhmet, Salima Cherkeshova and Gulbanu Zhiyenbayeva.; formal analysis, Maxat Tabylganov; investigation, Nursaule Tauova; resources, Anar Tlepbergenova; data curation, Gulbanu Zhiyenbayeva; writing—original draft preparation, Mansiya Yessenamanova; writing—review and editing, Zhanar Yessenamanova; visualization, Zhanar Yessenamanova; supervision, Kossarbay Kozhakhmet; project administration, Mansiya Yessenamanova; funding acquisition, Salima Cherkeshova. All authors have read and agreed to the published version of the manuscript.” The relevant terms are explained at the CRediT taxonomy.

Data Availability

The data of “Reserves attributable to the sites of the recommended wells” supporting our research results are included within the article or supplementary material.

Conflicts of Interest

The authors declare that they have no conflicts of interest.

References

- [1] M. S. Yessenamanova, L. K. Sangajieva, Z. S. Yessenamanova, and A. E. Tlepbergenova, “Migratory activity at the landfill site of microelements of the caspian depression,” *Series Geol. Tech. Sci.*, vol. 1, no. 439, pp. 155-163, 2020. <http://dx.doi.org/10.32014/2020.2518-170X.19>.
- [2] B. U. Haq and S. Schutter, “A chronology of paleozoic sea-level changes,” *Science*, vol. 322, no. 5898, pp. 64-68, 2008. <http://dx.doi.org/10.1126/science.1161648>.
- [3] “The main features of the geological structure and oil and gas potential of western Kazakhstan. Monograph. Leningrad. Publishing house: Gostoptehizdat. Proceedings of VNIGRI issue 213, pp. 61-91,” 1963. <https://bookree.org/reader?file=731245&ysclid=19v78ghfb857886741>.
- [4] S. M. Ozdoyev and M. A. Mashrapova, “Geological structure and methods of increasing oil recovery of the productive horizons of the Arystan deposit,” *News Natl. Acad. Sci. R.*, vol. 424, no. 4, pp. 270-275, 2017.
- [5] “The Triassic of the southern Mangyshlak,” Works of the All-Russian Research Oil Geological Institute, 1981, <https://www.geokniga.org/bookfiles/geokniga-trias-yuzhnogo-mangyshlaka-trudy-vyp-224-1981.pdf>.
- [6] S. M. Kan, E. Z. Murtazin, and A. M. Edilhanov, “About distribution rare microcomponents in passing stratal waters at the oil and gas fields of Peninsula Mangyshlak,” *News Natl. Acad. Sci. R.*, vol. 423, no. 3, pp. 84-94, 2017.
- [7] S. Saffarzadeh, A. Javaherian, H. Hasani, and M. A. Talebi, “Improving fault image by determination of optimum seismic survey parameters using ray-based modeling,” *J. Geophys. Eng.*, vol. 15, no. 3, pp. 668-680, 2018. <https://doi.org/10.1088/1742-2140/aaa044>.
- [8] B. Maksym and V. Kulyk, “Determination of basic gas reservoir parameters from radioactive logging taking

- into account PT-conditions,” *Nafta-Gaz*, vol. 3, 2017. <http://dx.doi.org/10.18668/NG.2017.03.03>.
- [9] T. R. Akhmedov, “3D seismic survey data processing and interpretation by use of latest tools applied for discovery of new traps in Pleistocene deposits of Hovsan field,” *AIMS Geosci.*, vol. 7, no. 1, pp. 95-112, 2021. <http://dx.doi.org/10.3934/geosci.2021005>.
- [10] S. M. Ozdoyev and M. A. Mashrapova, “Geological structure and methods of increasing oil recovery of the productive horizons of the arystan deposit,” *News Natl. Acad. Sci. R.*, vol. 4, no. 424, pp. 270-275, 2017.
- [11] J. C. Xu, H. Zhang, J. F. Zhang, Z. W. Li, and W. Liu, “Pre-stack time migration based on stationary-phase stacking in the dip-angle domain,” *J. Geophys. Eng.*, vol. 14, no. 2, pp. 272-282, 2017. <http://dx.doi.org/10.1088/1742-2140/aa576f>.
- [12] T. F. Lin, H. Deng, Z. F. Zhan, Z. H. Wan, and K. J. Marfurt, “Attributes assisted seismic interpretation in pre-stack time versus depth migration data,” In AAPG Annual Convention & Exhibition, Denver, CO, USA, 2015.
- [13] J. Cartwright and M. Huuse, “3D seismic technology: The geological ‘Hubble’,” *Basin Res.*, vol. 17, pp. 1-20, 2005. <https://doi.org/10.1111/j.1365-2117.2005.00252.x>.
- [14] N. Juhojuntti, G. Wood, C. Juhlin, C. Juhlin, C. O’Dowd, P. Dueck Peter, and C. Calin, “3D seismic survey at the Millennium uranium deposit, Saskatchewan, Canada: Mapping depth to basement and imaging post-Athabasca structure near the orebody,” *Geophysics*, vol. 77, no. 5, 2012. <http://dx.doi.org/10.1190/geo2012-0117.1>.
- [15] M. Manzi, G. R. J. Cooper, A. Malehmir, and R. J. Durrheim, “Integrated interpretation of 3D seismic data to enhance the detection of the gold-bearing reef: Mponeng Gold mine, Witwatersrand Basin (South Africa),” *Geophys. Prospect.*, vol. 63, no. 4, pp. 881-902, 2015. <http://dx.doi.org/10.1111/1365-2478.12273>.